Investigation of Phase Transitional Behavior of Poly(L-lactide)/ Poly(D-lactide) Blend Used to Prepare the Highly-Oriented Stereocomplex

Jianming Zhang,[†] Kohji Tashiro,*[,†] Hideto Tsuji,[‡] and Abraham J. Domb[§]

Department of Future Industry-oriented Basic Science and Materials, Graduate School of Engineering, Toyota Technological Institute, Tempaku, Nagoya 468-8511, Japan, Department of Ecological Engineering, Faculty of Engineering, Toyohashi University of Technology, Toyohashi, Aichi 441-8580, Japan, and Department of Medicinal Chemistry, School of Pharmacy-Faculty of Medicine, The Hebrew University of Jerusalem, Jerusalem 91120, Israel

Received July 26, 2006; Revised Manuscript Received September 16, 2006

ABSTRACT: By using the highly oriented 1:1 stoichiometric blend of high-molecular-weight PLLA and middle-molecular-weight PDLA species and by choosing a suitable annealing condition, we have succeeded for the first time to observe the phase transition phenomenon in the heating and cooling processes by measuring the temperature dependence of the X-ray fiber diagram and polarized IR spectra. The as-drawn sample was found to consist of the two crystalline phases; disordered α form (α′) and stereocomplex (β_c). In the heating process, the α′ form was found to be reorganized into the oriented α phase above 120 °C, which melted around 180 °C. However, by heating this sample some more, some parts of the molten chains are found to crystallize on the surface of the β_c crystallites with high degree of chain orientation. In the subsequent cooling process from the β_c phase, the unoriented α crystal appeared at around 120 °C and coexisted with the highly oriented β_c crystals.

Introduction

In the past few decades, polylactide (PLA) (−[CH(CH_3)-COO]$_n$−) has been attracting great attention, because it is producible from annually renewable natural sources, such as corn and potatoes.[1] Due to the presence of a carbon chiral center in the skeletal chain, two enantiomers of PLA, poly(L-lactide) (PLLA) and poly(D-lactide) (PDLA), have been synthesized. Usually, it is known that PLA homopolymer (PLLA or PDLA) can form three kinds of crystal modifications (α, β and γ).[2−5] Very recently, several authors proposed that the existence of another crystal modification, the α′ form or disorder α on the basis of X-ray powder diffraction and infrared spectroscopic study.[6,7] As discussed in our previous paper,[8] the α′ phase can be distinguished definitely from the α phase by comparing the X-ray fiber diagrams and polarized IR/Raman spectra. For example, Figure 1a shows the X-ray fiber diagrams of the α′ and α forms taken for uniaxially oriented PLLA samples. Their difference can be seen clearly from the comparison of the X-ray diffraction profiles along the sixth and seventh layer lines as shown in Figure 1b. The pure α′ phase can be prepared by annealing the oriented sample in the temperature region between 60 °C (T_g) and 120 °C, while the pure α phase is obtained above 120 °C. The preliminary study of the X-ray diffraction data suggests that the α′ phase might be characterized with the disordered chain packing or the disordered helical conformation, though the details have not yet been clarified at all.

The stereocomplex of PLLA and PDLA is another important crystal modification of PLA. Since Ikada et al.[9] and Murdoch et al.[10] found a stereocomplex formation from equimolar mixtures of PLLA and PDLA both in melt and solutions, numerous studies have been performed on the formation and crystallization of the stereocomplex as well as its crystalline structure, morphology and physical properties.[11−20] PLA stereocomplexation can take place both for enantiomeric PLA-based homopolymers and for a linear or star block copolymer consisting of L- and D-lactide sequences.[14−17] One of the most characteristic features of the PLA stereocomplex is its high melting point, higher by 50 °C than that of the original parent polymer components.[9,17] To understand this distinct property, one needs to study the crystal structure and intermolecular interactions between PLLA and PDLA.[18−22]

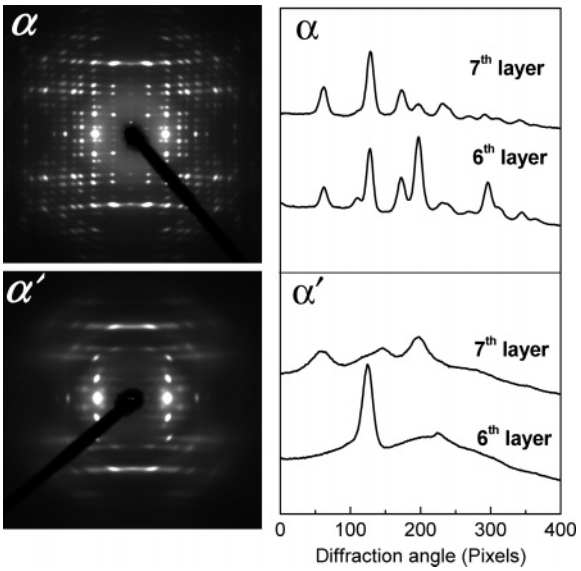

Figure 1. (a) X-ray fiber diagrams and (b) comparison of the one-dimensional profiles along the sixth and seventh layer lines evaluated from part a of uniaxailly oriented PLLA α and α′ crystals.

* To whom all correspondence should be addressed. Fax: (+81) 52809 1721. E-mail: ktashiro@toyota-ti.ac.jp.

† Department of Future Industry-oriented Basic Science and Materials, Graduate School of Engineering, Toyota Technological Institute.

‡ Department of Ecological Engineering, Faculty of Engineering, Toyohashi University of Technology.

§ Department of Medicinal Chemistry, School of Pharmacy-Faculty of Medicine, The Hebrew University of Jerusalem.

10.1021/ma061693s CCC: $37.00
Published on Web 01/25/2007

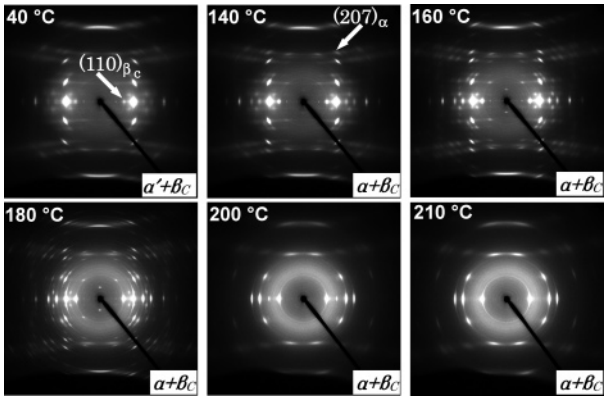

Figure 2. X-ray fiber diagrams of as-drawn PDLA/PLLA blend rod taken at elevated temperatures. The vertical axis is along the draw direction.

Unfortunately, however, the structure of the stereocomplex has not yet been clarified enough satisfactorily. This is because of the lack of an X-ray fiber pattern and/or the polarized IR/Raman spectra of the uniaxially oriented PLA stereocomplex. These fundamental data should be very important and useful for solving the question mentioned above because the polarized IR/Raman spectra are helpful for making accurate band assignments, being the prerequisite conditions for studying the intermolecular interactions between PLLA and PDLA by vibrational spectroscopy. The 2-dimensional X-ray fiber diagram is also indispensable for the detailed structural study, because the equatorial and layer line reflections can be separated well and the ambiguous interpretation encountered frequently for the powder X-ray diffraction data of the unoriented sample can be avoided. The equimolar blending of PDLA and PLLA of low molecular weights ($<1 \times 10^5$ g/mol) is said to be a favorable condition for exclusive formation of stereocomplex crystallites without any additional formation of homocrystallites.[23] However, an unoriented stereocomplex sample prepared from such a low-molecular-weight species is very brittle and hard to stretch to high degree of orientation.

In the present study, by using asymmetric 1:1 blend of PLLA and PDLA with different molecular weights and by choosing suitable annealing conditions, we have succeeded in preparing the highly oriented and highly crystalline PLA stereocomplex. The X-ray fiber pattern and polarized IR/Raman spectra of the PLLA/PDLA stereocomplex were successfully obtained for the first time. We report the details of the preparation conditions of highly oriented and crystalline PLLA/PDLA stereocomplex. Additionally we describe also the phase transitions occurring in the heating process of the thus-prepared PLLA/PDLA blend sample, from which structural characteristics of the phase transition can be extracted clearly and at the same time the concrete conditions necessary for getting the pure stereocomplex can be deduced reasonably.

Experimental

Material and Preparation Procedures. The synthesis and purification of PLLA and PDLA samples used in this study were performed according to the procedures reported previously.[24] For PLLA, the weight-averaged molecular weight (M_w) was 8.4×10^5 g mol^{-1} and the number-average molecular weight (M_n) was 3.6×10^5. For PDLA, M_w was 7.7×10^4 g mol^{-1} and M_n was 5.2×10^4. The PLLA and PDLA samples were dissolved into chloroform at 1:1 weight ratio and the films were obtained by casting on a glass slide at room temperature. The samples were melted and quenched into ice water to obtain the amorphous samples. The rectangular strip of the amorphous sample was stretched by 4 times the original length in oil bath at 85 °C, which was above the glass transition temperature of PLA (ca. 58 °C). The thus prepared oriented samples were annealed at a suitable temperature to get the highly oriented stereocomplex without any traces of homocrystallites. Detailed annealing conditions are described later.

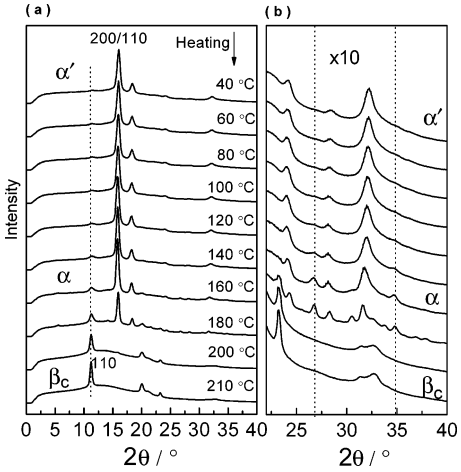

Figure 3. (a) X-ray diffraction profiles of the PLLA/PDLA blend sample obtained from circularly integrated intensities of the fiber diagrams shown in Figure 2. (b) Enlarged profiles in a higher diffraction angle region.

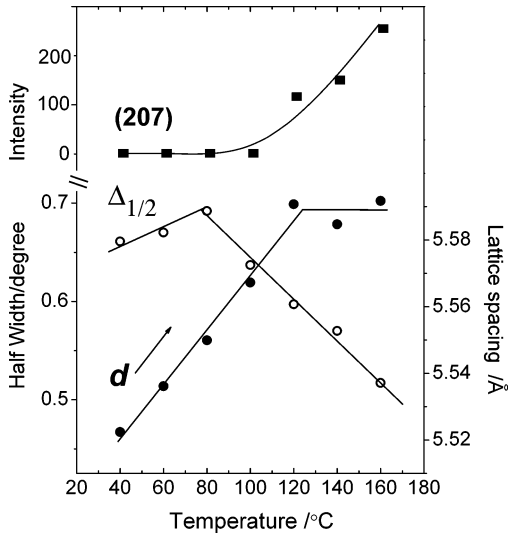

Figure 4. Temperature dependence of the intensity of (207) reflection, peak width and lattice spacing estimated for the (200)/(110) reflection of the α (α′) form.

The pure α′ and α forms were prepared by annealing the oriented PLLA samples in oil bath at 85 and 150 °C for 3 h, respectively.

Measurements. In the preparation process for the highly oriented stereocomplex, the annealing temperature was found to be important for getting an almost pure stereocomplex without the homocrystallites. To investigate the more concrete conditions, we performed the temperature dependent measurement of the X-ray diffraction pattern for the as-drawn sample in the heating and cooling processes. The sample was set into a homemade heater, which was mounted on the goniometer head of an X-ray apparatus. The fiber diagrams were recorded using an imaging plate system DIP 1000 (MAC Science Co. Japan) with the graphite-monochromatized Cu Kα line as the incident X-ray beam ($\lambda = 1.54$ Å).

Polarized infrared spectra were measured with a Varian FTS-7000 Fourier-transform infrared spectrometer equipped with a wire-grid polarizer. The resolution powers for the IR were 2 cm^{-1}. The thermograms were measured at the heating rate 10 °C/min using a TA Instruments DSC Q1000.

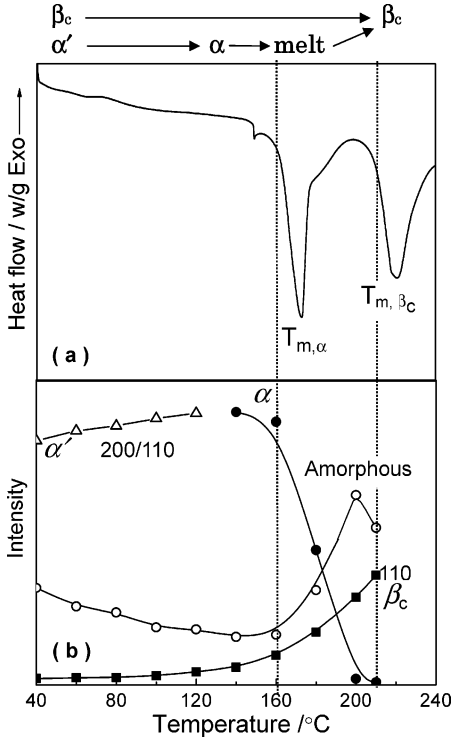

Figure 5. (a) DSC curve of as-drawn PDLA/PLLA blend in the first heating process (b) Comparison of the integrated intensity change of amorphous halo, the (200)/(110) reflection of PLA homocrystallites, and the strongest reflection of the PLLA/PDLA stereocomplex.

Results and Discussion

Factors Necessary for Preparing Uniaxially Oriented Stereocomplex. Stereocomplexation of the PDLA/ PLLA blend occurs usually during the crystallization in the solution or in the cooling procedure from the melt, which are also the crystallization conditions for the α form of PLA homopolymer. It means that there is a competition between the crystallization of stereocomplex crystallite and that of PLA homocrystallites in the blend system of PLLA and PDLA. It has been reported that the most common conditions required for exclusive formation of stereocomplex crystallites without formation of any homocrystallites include the following: (1) equimolar blending of D-lactide and L-lactide units,[9] (2) low molecular weights for both the isomeric polymers (there exists an upper critical molecular weight, about 1×10^5 g/mol, below which the formation of stereocomplex can occur in bulk from the melt or in the solution[23]), and (3) sufficiently high stereoregularity for both PLLA and PDLA.[25,26] In short, the 1:1 blend of low-molecular-weight PLLA and PDLA is desired for the stereocomplex formation.

However, the stereocomplex consisting of such low-molecular-weight components is very brittle and cannot be easily stretched. Usually, a high-molecular-weight polymer is needed for preparing the highly oriented sample. By considering these two opposite demands, we used the stoichiometric 1:1 blend of PLLA and PDLA with different molecular weights. That is, the high-molecular-weight PLLA and the middle-molecular-weight PDLA were used where the molecular weights were, respectively, higher and lower than the above-mentioned critical molecular weight (1×10^5 g/mol). Using such a blend system, we succeeded to prepare the highly oriented L/D blend by stretching 4 times the original length. The thus prepared samples were found to contain both the α′ (disordered α) and the stereocomplex (β_c) (For convenience and distinguishing from the β form of PLA homocrystal, we named the PLLA/PDLA

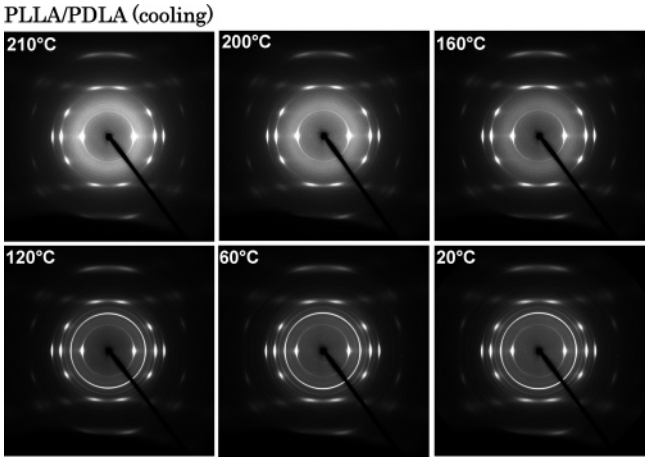

Figure 6. X-ray fiber patterns of the as-drawn PDLA/PLLA blend in the cooling process. The vertical axis is along the draw direction.

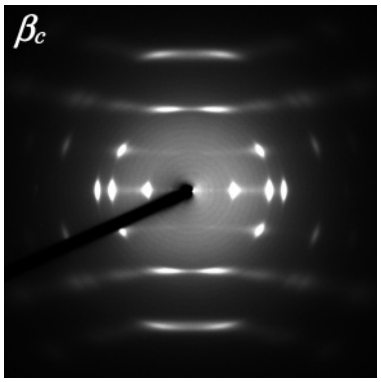

Figure 7. X-ray fiber pattern of the PLLA/PDLA stereocomplex at room temperature. The vertical axis is along the draw direction.

complex β_c). For improving the purity of L/D stereocomplex and erasing the PLA homocrystallites, it was important to find out a suitable annealing temperature. Then, we performed the temperature-dependent measurement of the X-ray diffraction pattern in the heating and cooling processes for the as-drawn PLLA/PDLA blend sample.

Temperature-Dependent X-ray Measurements. The X-ray fiber diagrams of the as-drawn PDLA/PLLA blend sample measured in the heating process are shown in Figure 2. At 40 °C, the sample mainly contains the oriented homocrystallites: the X-ray pattern is essentially the same as that of the disorder α form of PLA (α′) as shown in Figure 1. But, as indicated by an open arrow, we can observe also the (110) reflection originating from the stereocomplex,[5] the relative intensities of which are weaker than those of the α′ form. With increasing the temperature to 140 °C, the reflections of the α′ form changed into those of the α form. Typical change was detected for the reflections on the seventh layer. The seventh layer reflections became clearer at 160 °C. Essentially the same change in X-ray fiber diagram is observed in the case of PLA homopolymer.[8] As already reported, the X-ray fiber diagram of the as-drawn PLLA sample shows the diffuses and weak seventh layer reflections, which become strong and much clearer above 120 °C. In the previous paper, we interpreted this diffraction pattern change in terms of the disorder-to-order transition from the α′ to the α form.[8] This concept can explain the unusual crystallization behavior of PLA homopolymer reasonably as pointed out by Zhang et al.[6,7] That is, the curve of PLLA spherulite growth rate (G) vs crystallization temperature (T_c), shows a discontinuity around 100−120 °C and

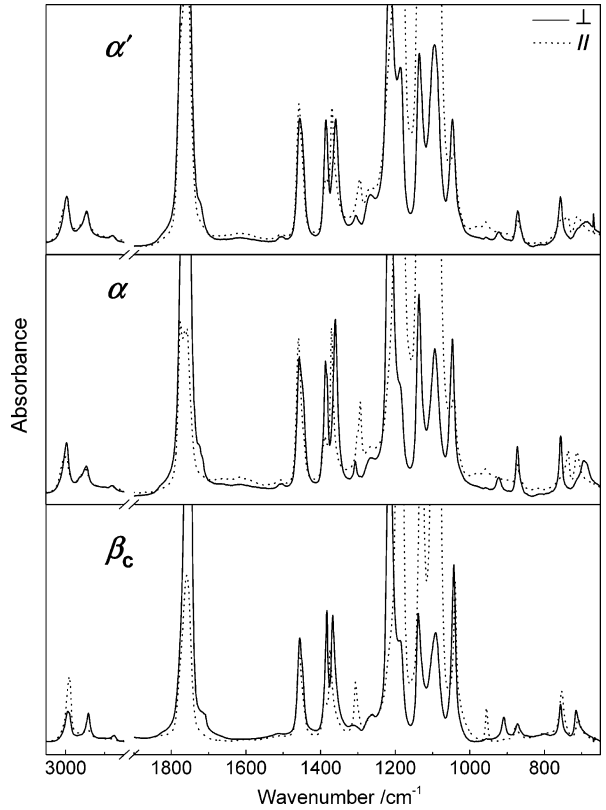

Figure 8. Polarized IR spectra of uniaxially oriented PLA α′, α, and β_c forms.

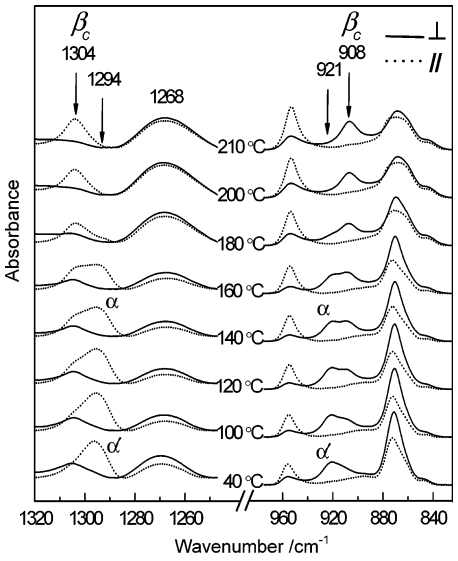

Figure 9. Temperature dependence of the polarized infrared spectra in the frequency region 1320−825 cm^{-1} measured for the uniaxially oriented PLLA/PDLA blend film.

deviates from the bell-shaped curve usually observed in the spherulite growth. This discontinuous change comes from the difference of crystalline state between the α′ and α forms. The X-ray diagram change observed for PDLA/PLLA blend is just the same as that of PLLA homopolymer. Therefore, we may say that the disorder-to-order transition occurred from α′ to α in the temperature region higher than 120 °C. When the temperature reached 180 °C, higher than the melting point of the PLA α form (ca. 175 °C), most of the reflections of the α form disappeared due to the melt and the amorphous halo become clearer. At the same time, the reflections of the L/D

Table 1. Infrared Bands Characteristic of PLA α′, α, and β_c forms

α′/cm^{-1}	α/cm^{-1}	polarization[a]	β_c/cm^{-1}	polarization[a]
1458	1458	∥	1455	⊥
1386	1387	⊥	1383	⊥
	1382			
1371	1371	∥	1374	∥
1359	1359	⊥	1368	⊥
1294	1393	∥	1306	∥
	1302			
958	958	∥	954	∥
922	922	⊥	908	⊥
872	872	⊥	872	⊥
756	756	⊥	755	∥
736	736	∥	756	⊥
712	712	∥	715	⊥
690	690	⊥	709	∥

[a] ∥ and ⊥ indicate that the electric vector of incident infrared beam is parallel and perpendicular to the chain direction, respectively.

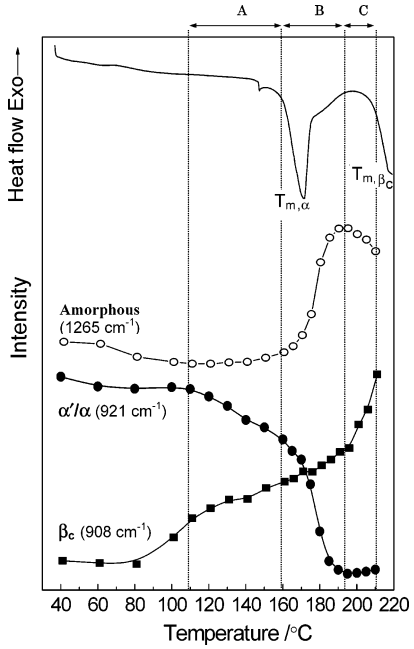

Figure 10. Integrated intensity of the characteristic IR bands of amorphous region (1268 cm^{-1}), α (921 cm^{-1}), and β_c (908 cm^{-1}) phases for the uniaxially oriented PLLA/PDLA blend film as a function of the temperature. For comparison, the corresponding DSC curve is also displayed.

stereocomplex became stronger. At 210 °C, the homocrystallites disappeared totally and only the pure stereocomplex was left. The melting point of PLA stereocomplex is around 230 °C. In order to keep the state of the stereocomplex after cooling down to room temperature, the heating was stopped at this temperature.

Figure 3 shows the temperature dependence of the X-ray diffraction profiles obtained from circularly integrated intensities of the fiber diagrams shown in Figure 2. The two strongest peaks around $2\theta = 16.0°$ and 18.4°, as seen in Figure 3a, are the characteristic reflections of PLA homocrystallites (α′ and α forms). With increasing temperature above 120 °C, several new diffraction peaks start to appear in higher diffraction angle region as demonstrated in the enlarged profiles (Figure 3b), corresponding to the transition from the α′ to the α phase. The three peaks around $2\theta = 11.1°$, 20.0°, and 23.2° observed above 180 °C correspond to the reflection characteristics of PLA stereocomplex (β_c).

As mentioned already in Figure 2, the seventh layer reflections become stronger and clearer above 120 °C, indicating the disorder-to-order transition from α′ to α form. For making the

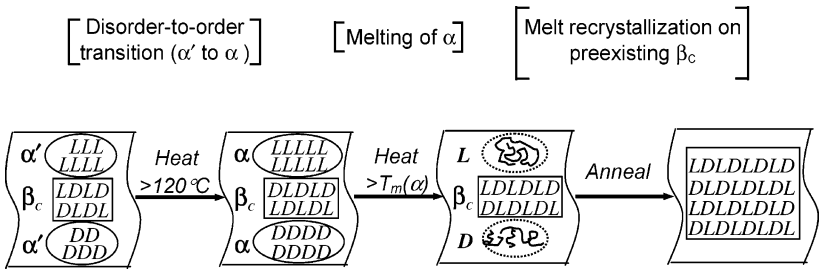

Figure 11. Schematic illustration of the regularization from α′ to α form, the melt of the α form, and the recrystallization/epitaxial growth into the oriented β_c form in the heating process of PLLA/PDLA blend sample.

disorder-to-order transition temperature clear, the intensity of the (207) reflection on the seventh layer is plotted against temperature in Figure 4 together with the half-width and lattice spacing of the strongest (200)/(110) reflection. When the temperature is above 80 °C, which is to some extent higher than the glass transition temperature of PLA homopolymer (ca. 58 °C), the half-width starts to decrease linearly with temperature. The decrease in the reflection width indicates that the crystallites are larger in the heating process from 80 to 160 °C. Below 120 °C, the lattice spacing linearly increases with increasing temperature, corresponding to the thermal expansion of the PLA homocrystallites. The lattice spacing of the (200)/(110) plane is almost constant above 120 °C, just where the seventh layer reflections start to appear and increase in intensity and the phase transition occurs from the α′ to the α form.

The temperature dependence of the integrated intensity of the reflection characteristic of the α′ and α forms and that of the stereocomplex (β_c) are compared with the DSC thermogram as shown in Figure 5. In this figure the relative intensity of the amorphous halo is also plotted. (The intensity estimated is a peak height at the fixed scattering angle, not the integrated intensity. This is because the curve fitting procedure could not give us unique answer due to too many fitting parameters. But, anyway, the peak height may be used here reasonably as a measure to represent the change in the relative amount of the molten region qualitatively.) In the temperature region 160−200 °C, the relative amount of α homocrystallites decreased drastically. The intensity of the halo peak increased at the same time. The reflection intensity of the β_c form increased in this temperature region. Above 200 °C the intensity of the halo turned to decrease while that of the β_c form continued to increase. From the correspondence between these X-ray reflection changes and the DSC thermogram, we may assign the DSC peaks to the transitions indicated in Figure 5. Around 200 °C the partial change of the amorphous phase into the β_c form occurs as known from the decrease in halo intensity and the increase in the β_c reflection. It should be noted here that the orientation of the chains is kept unchanged during the transition as seen in the 2-dimensional X-ray diagram of Figure 2. Therefore, some parts of the molten chains are considered to crystallize on the surface of the oriented β_c crystallites with the high degree of chain orientation along the *c*-axis of the preexisting crystallites.

When the sample is cooled from 210 °C, the X-ray Debye−Scherrer rings of the unoriented α form appear at 120 °C and are coexistent with the reflections of the oriented stereocomplex as shown in Figure 6. The X-ray fiber pattern obtained at 20°C after slow cool from 210 °C consists of the pattern of oriented β_c and the pattern of unoriented α form. By annealing the oriented blend at high temperature between the melting points of α (175 °C) and β_c (230 °C) for a long time and subsequently quenching the sample quickly to room temperature, we can get the X-ray diffraction of pure and highly oriented stereocomplex without any traces of homocrystallites as shown in Figure 7. In this way, we have found a method to prepare the highly oriented and pure β_c sample for the first time.

Polarized IR Spectra. Once we know the method to get the pure crystal forms of α′, α, and β_c for the PLA and PLLA/PDLA blend samples, we could take the polarized IR and Raman spectra of these crystal forms. Figure 8 shows the polarized IR spectra of α′, α, and β_c forms, as examples. In the whole spectral region of the polarized IR spectra, the α and α′ forms are highly similar to each other, indicating the similar chain conformation of these two forms. In contrast, the polarized IR spectra of the β_c are obviously different from those of α and α′ forms. There are many bands to be observed at different positions between β_c and α (α′) forms.

Table 1 summarizes the IR spectral features of α, α′, and β_c forms, which are useful as a guiding principle for the identification of these crystalline forms. In the spectral region of 975−825 cm^{-1}, the perpendicular bands at 908 and 921 cm^{-1}, assigned to the coupling of C−C backbone stretching with the CH_3 rocking mode, are sensitive to the chain conformation of PLA.[27−29] It was reported that the β form of PLLA homocrystal and the β_c form of PLA stereocomplex have essentially the same 3/1 helical conformation and show the characteristic bands at 912 and 908 cm^{-1}, respectively.[18,19,29] On the other hand, the α′ and α forms of 10/3 helical conformation shows the characteristic band at 921 cm^{-1}.[2,30,27−29]

Temperature-Dependent IR Measurements. In order to clarify the phase transitional behavior of the uniaxially oriented PLA D/L blend in the heating process from the vibrational spectroscopic point of view, we performed the temperature-dependent IR measurement. The uniaxially oriented L/D blend sample was sandwiched between a pair of KBr plates. The IR spectra were measured every 10 °C in the heating process after holding for 30 min until reaching the thermal equilibrium. Figure 9 shows the temperature dependence of the polarized infrared spectra in the frequency region of 1320−825 cm^{-1} measured for the uniaxially oriented PLLA/PDLA blend film. The bands characteristic of the α form decrease in intensity around 180 °C and those of the β_c form increase instead. It should be noted that both the bands of the α (α′) and β_c show clear dichroism even in the melting temperature region of the α form, consistent with the 2-dimensional X-ray pattern given in Figure 2.

The intensities of the characteristic bands of the amorphous region (1268 cm^{-1}), α (921 cm^{-1}) and β_c (908 cm^{-1}) phases together with the DSC curve are plotted as a function of temperature in Figure 10. Consistently with the X-ray diffraction data, the transitions from the α′ to α and the α to melt are observed clearly in the temperature regions A and B indicated in Figure 10. It should be noticed here the α′-to-α phase transition occurs with the infrared polarization kept almost perfectly, while the polarization disappears in the α-to-melt

transition. In the temperature region of C, the amorphous band decreases again and the infrared band of the β_c increases in intensity with keeping the dichroic ratio clearly. That is to say, some parts of the molten region are crystallized into the β_c crystallites. As known from the reservation of the chain orientation in the melt to β_c transition, the recrystallization of the amorphous chains is considered occur with keeping the chain orientation on the surface of the β_c crystallites. In this way, both the infrared and X-ray data clarify the phase transition consistently.

A schematic illustration of the transition behavior between the α′, α, melt and β_c forms is given in Figure 11. Before the melting point of PLA homocrystallites of α form, there exist three kinds of crystal lamellae: homocrystallites (α′) of PLLA and PDLA and L/D stereocomplex (β_c). The α′ form transforms to the more regular α form around 120 °C in both the L and D crystallites. However, the α form is melted in the region of 170 to 190 °C. By heating the sample furthermore some parts of the molten chains are found to migrate onto the surface of the β_c crystallites, resulting in the further growth of the β_c crystallites. In particular, the preservation of chain orientation in the β_c form, as revealed by the X-ray fiber pattern and polarized infrared spectra, indicate the oriented crystal growth occurs on the surface of the preexisting β_c crystallites. In this temperature region, only the oriented β_c is left. By quenching the sample at this stage to the room-temperature quickly, the pure and highly oriented β_c crystal could be obtained. When cooled slowly from this region, on the other hand, a mixture of oriented β_c and unoriented α forms is obtained.

Conclusion

So far it was quite difficult to prepare the pure and highly oriented stereocomplex (β_c) of PLLA/PDLA blend. As reported in the present paper, we have been able to clarify the preparation condition of highly oriented β_c form for the first time. One key point is to use the 1:1 stoichiometric blend of high-molecular-weight PLLA and middle molecular weight PDLA. Another key point is to choose the annealing temperature, i.e., the temperature region between the melting points of α and β_c forms. In this paper, we have clarified also the phase transition behavior of PLLA/PDLA blend sample by performing the temperature-dependent measurement of the X-ray fiber diagram and infrared spectra. The structurally disordered α′ form contained in the starting sample was found to regularize into the order α form above 120 °C. This phenomenon itself is essentially the same as that observed for the α′ form of the PLA homopolymer. As known from the comparison of DSC thermogram with the temperature dependence of X-ray and infrared spectral data, the transition of the α to the β_c form does not occur as the solid-to-solid transition but the α form melts at first and then the melt recrystallizes into the β_c form (α-to-melt-to-β_c). However, the chain orientation is almost perfectly kept during this melt-recrystallization process. A more detailed investigation of this orientation growth is now being made. Once the pure and highly oriented β_c sample can be obtained, we can measure the physical properties of the β_c crystal. In particular, the question why the melting point of β_c crystal is overwhelmingly higher than that of the α form may be solved definitively.

Acknowledgment. This work was supported by MEXT "Collaboration with Local Communities" Project (2005-2009).

References and Notes

(1) Ikada, Y.; Tsuji, H. *Macromol. Rapid Commun.* **2000**, *21*, 117−132.
(2) Hoogsteen, W.; Postema, A. R.; Pennings, A. J.; ten Brinke, G.; Zugenmaier, P. *Macromolecules* **1990**, *23*, 634−642.
(3) Kalb, B.; Pennings, A. J. *Polymer* **1980**, *21*, 607−612.
(4) Puiggali, J.; Ikada, Y.; Tsuji, H.; Cartier, L.; Okinara, T.; Lotz, B. *Polymer* **2000**, *41*, 8921−8930.
(5) Cartier, L.; Okihara, T.; Ikada, Y.; Tsuji, H.; Puiggali, J.; Lotz, B. *Polymer* **2000**, *41*, 8909−8919.
(6) Zhang, J. M.; Duan, Y. X.; Sato, H.; Tsuji, H.; Noda, I.; Yan, S.; Ozaki, Y. *Macromolecules* **2005**, *38*, 8012−8021.
(7) Cho, T.-Y.; Strobl, G. *Polymer* **2006**, *47*, 1036−1043.
(8) Zhang, J. M.; Tashiro, K.; Domb, A. J.; Tsuji, H. *Macromol. Symp.* **2006**, *242*, 274−278.
(9) Ikada, Y.; Jamshidi, K.; Tsuji, H.; Hyon, S.-H. *Macromolecules* **1987**, *20*, 904−906.
(10) Murdoch, J. R.; Loomis, G. L. U.S. Patent 4,719,246, 1988.
(11) Slager, J.; Domb, A. J. *Adv. Drug Delivery Rev.* **2003**, *55*, 549−583.
(12) Tsuji, H. *Macromol. Biosci.* **2005**, *5*, 569−597.
(13) Fukushima, K.; Kimura, Y. *Polym. Int.* **2006**, *55*, 626−642.
(14) Li, L. B.; Zhong, Z. Y.; de Jeu, W. H.; Dijkstra, P. J.; Feijen, J. *Macromolecules* **2004**, *37*, 864 − 8646.
(15) Yui, N.; Dijkstra, P. J.; Feijen, J. *Makromol. Chem.* **1990**, *191*, 481−488.
(16) Spassky, N.; Pluta, C.; Simic, V.; Thiam, M.; Wisniewski, M. *Macromol. Symp.* **1998**, *128*, 39.
(17) Biela, T.; Duda, A.; Penczek, S. *Macromolecules* **2006**, *39*, 3710−3713.
(18) Okihara, T.; Tsuji, M.; Kawaguchi, A.; Katayama, K.-I.; Tsuji, H.; Hyon, S.-H.; Ikada, Y. J. *Macromol. Sci., Phys.* **1991**, *B30*, 119−140.
(19) Cartier, L.; Okihara, T.; Lotz, B. *Macromolecules* **1997**, *30*, 6313−6322.
(20) Brizzolara, D.; Cantow, H.-J.; Diederichs, K.; Keller, E.; Domb, A. J. *Macromolecules* **1996**, *29*, 191−197.
(21) Zhang, J. M.; Sato, H.; Tsuji, H.; Noda, I.; Ozaki, Y. *Macromolecules* **2005**, *38*, 1822−1828.
(22) Sarasu, J. R.; Rodriguez, N. L.; Arraiza, A. L.; Meaurio, E. *Macromolecules* **2005**, *38*, 8362−8371.
(23) Tsuji, H.; Hyon, S.-H.; Ikada, Y. *Macromolecules* **1991**, *24*, 5651−5656.
(24) Tsuji, H. Ikada, Y. *Polymer* **1999**, *40*, 6699−6708.
(25) Tsuji, H.; Ikada, Y. *Macromolecules* **1992**, *25*, 5719−5723.
(26) Brochu, S.; Prud'homme, R. E.; Barakat, I.; Jerome, R. *Macromolecules* **1995**, *28*, 5230−5239.
(27) Kister, G.; Cassanas, G.; Vert, M. *Polymer* **1998**, *39*, 267−273.
(28) Sawai, D.; Takahashi, K.; Sasashige, A.; Kanamoto, T. *Macromolecules* **2003**, *36*, 3601−3605.
(29) Aou, K.; Hsu, S. L. *Macromolecules* **2006**, *39*, 3337−3344.
(30) Aleman, C.; Lotz, B.; Puiggali, J. *Macromolecules* **2001**, *34*, 4795−4801.

MA061693S